Journal of Thermal Analysis and Calorimetry, Vol. 80 (2005) 201–206

TEMPERATURE-PROGRAMMED DESORPTION (TPD) OF CARBON DIOXIDE ON ALKALI-METAL CATION-EXCHANGED FAUJASITE TYPE ZEOLITES

O. Klepel[1] *and B. Hunger*[2*]

[1]Institut für Technische Chemie, Universität Leipzig, 04103 Leipzig, Germany
[2]Wilhelm-Ostwald-Institut für Physikalische und Theoretische Chemie, Universität Leipzig, 04103 Leipzig, Germany

Using temperature-programmed desorption (TPD), we have investigated the interaction of carbon dioxide with alkali-metal cation-exchanged faujasite type zeolites (LSX, X and Y). TPD in the temperature range between 300 and 500 K results in desorption profiles of different intensities depending on the kind of cation and the aluminium content of zeolites. For NaX the desorbed amount corresponds to about one percent of the saturation capacity at 298 K. In case of NaX and X type zeolites exchanged with Cs^+ ions an additional desorption peak above 500 K could be observed. Taking into account desorption curves of different heating rates, desorption energy distribution functions were calculated by using an extended integral equation. Initial adsorbed CO_2 could be assigned to carbonate species in different environments by DRIFT spectroscopy.

Keywords: *adsorption of CO_2, carbonate species, DRIFTS, faujasite type zeolites, TPD*

Introduction

In many industrial processes like air separation, hydrogen production and helium extraction carbon dioxide needs to be removed from various gas mixtures. Different types of alkali-metal cation-exchanged zeolites are suitable adsorbents for CO_2 (e.g. [1–11]). Moreover, CO_2 is widely used as a probe molecule to study properties of basic surface sites of metal oxides and zeolites (e.g. [12–14]). For both applications the best possible characterization of the carbon dioxide adsorption and desorption characteristics of the studied metal oxides and zeolites, respectively, is required. The temperature-programmed desorption (TPD) is an appropriated method to obtain detailed information about the adsorption/desorption behavior in particular considering low adsorbate concentrations. This should be an advantage in comparison to isothermal adsorption measurements, where low coverages are relatively difficult to investigate, because of very low equilibrium pressures.

Therefore, we have studied the temperature-programmed desorption of carbon dioxide on alkali-metal cation-exchanged faujasite type zeolites (LSX, X and Y) after adsorption of CO_2. Different experimental adsorption conditions (adsorption time, temperature) were applied. The TPD results were interpreted by means of diffuse reflectance infrared Fourier transform spectroscopic (DRIFTS) measurements.

Experimental

Zeolites

The parent faujasite samples NaX and NaY, both supplied from the Chemie AG Bitterfeld/Wolfen (Germany), were ion-exchanged with aqueous solutions of KCl, RbCl and CsCl as described elsewhere [15, 16]. Furthermore, a Li-LSX zeolite produced by Tricat Zeolites GmbH, Bitterfeld (Germany) was also studied. The micropore volumes were determined by nitrogen adsorption at 77 K (*t*-plot analysis). The characteristics of all studied zeolites are summarized in Table 1.

Temperature-programmed desorption (TPD)

All TPD experiments were carried out in a flow apparatus with helium as carrier gas (50 cm^3 min^{-1}). For evolved gas detection both a thermal conductivity detector (TCD) and a quadrupole mass spectrometer (Leybold, Transpector CIS System) with a capillary-coupling system were used. The zeolite samples were equilibrated with water vapor over a saturated $Ca(NO_3)_2$ solution in a desiccator. For each experiment 500 mg of hydrated zeolite were used in a mixture with 1 g quartz of the same grain size (0.2–0.4 mm). The zeolites were heated up to 773 K at 10 K min^{-1} in a helium flow. In the following step the samples were cooled down to adsorption temperature (300–450 K) and loaded with carbon dioxide. The saturated samples were flushed with helium at several times (0.5–7 h). Afterwards the linear

* Author for correspondence: hunger@chemie.uni-leipzig.de

1388–6150/$20.00

Akadémiai Kiadó, Budapest, Hungary
Springer, Dordrecht, The Netherlands

Table 1 Zeolite characteristics

Zeolite	Si/Al	Chemical composition	Micropore volume/$cm^3\ g^{-1}$
Li-LSX	1.01	$Li_{93.1}Na_{2.4}[Al_{95.5}Si_{96.5}O_{384}]$	0.309
NaX	1.18	$Na_{88.1}[Al_{88.1}Si_{103.9}O_{384}]$	0.295
KNaX	1.18	$K_{66.1}Na_{22}[Al_{88.1}Si_{103.9}O_{384}]$	0.263
RbNaX	1.35	$Rb_{57.8}Na_{23.9}[Al_{81.7}Si_{110.3}O_{384}]$	0.217
CsNaX(5)	1.18	$Cs_{4.4}Na_{83.7}[Al_{88.1}Si_{103.9}O_{384}]$	0.231
CsNaX(45)	1.18	$Cs_{39.6}Na_{48.5}[Al_{88.1}Si_{103.9}O_{384}]$	0.194
CsNaX(55)	1.35	$Cs_{44.9}Na_{36.8}[Al_{81.7}Si_{110.3}O_{384}]$	0.201
NaY	2.6	$Na_{53.3}[Al_{53.3}Si_{138.7}O_{384}]$	0.296
CsNaY	2.6	$Cs_{35.5}Na_{17.8}[Al_{53.3}Si_{138.7}O_{384}]$	0.196

temperature program (10 K min^{-1}) was started. The desorbed amounts of carbon dioxide were determined by calibration of the intensity of 44 amu response. Experiments with different heating rates (α=2–20 K min^{-1}) were carried out for a quantitative analysis of the desorption profiles.

DRIFT spectroscopic studies

The DRIFT spectroscopic experiments were carried out with a System 2000R spectrometer (Perkin Elmer) using a Praying Mantis diffuse reflection attachment equipped with a stainless steel reaction chamber (Harrick) allowing temperature-programmed investigations between room temperature and 723 K in a carrier gas flow (helium, 50 $cm^3\ min^{-1}$). For each experiment about 50 mg of hydrated NaX zeolite (granulated, 0.2–0.4 mm) were used. At first the zeolites were heated up to 673 K at 10 K min^{-1} in a helium flow. Afterwards the samples were cooled down to 298 and 413 K, respectively, and loaded with carbon dioxide in a CO_2/He flow (3.3 vol%). In the following step zeolites were flushed with helium at several times (30–60 min). The spectra were recorded at a resolution of 4 cm^{-1} with 32 scans being averaged. KBr was used as standard (background).

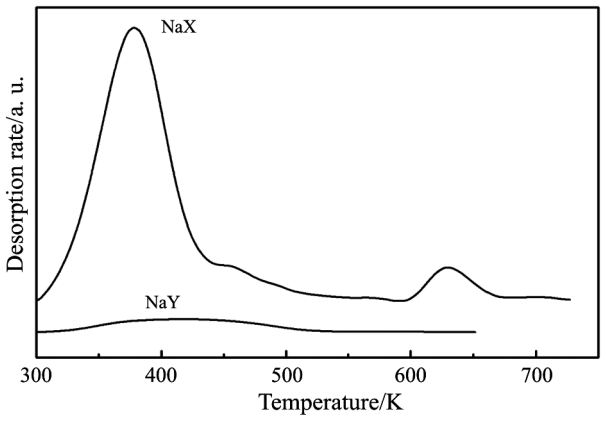

Fig. 1 Desorption profiles of CO_2 on NaX and NaY (10 K min^{-1})

Results and discussions

Figures 1–3 show the desorption profiles of all investigated zeolites which were obtained after adsorption of carbon dioxide at 298 K. The desorbed amounts are summarized in Table 2. In case of NaY, Li-LSX and CsNaY zeolites a very small CO_2 uptake was found for the used adsorption conditions. The other zeolites show a pronounced peak at around 370–390 K of different intensities and a weak shoulder at higher temperatures (470–480 K). For the NaX zeolite the desorbed amount corresponds to about one percent of the saturation capacity at 298 K (e.g. [5, 10, 17]).

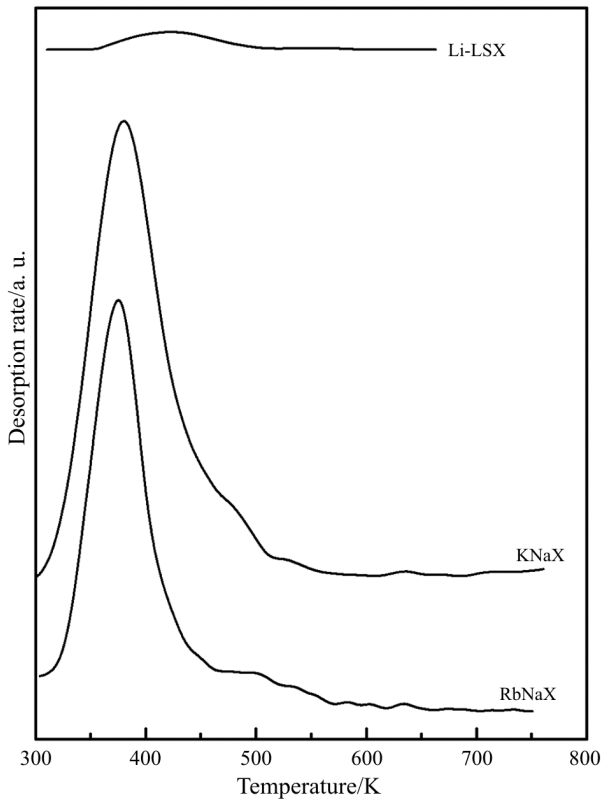

Fig. 2 Desorption profiles of CO_2 on Li-LSX, KNaX and RbNaX (10 K min^{-1})

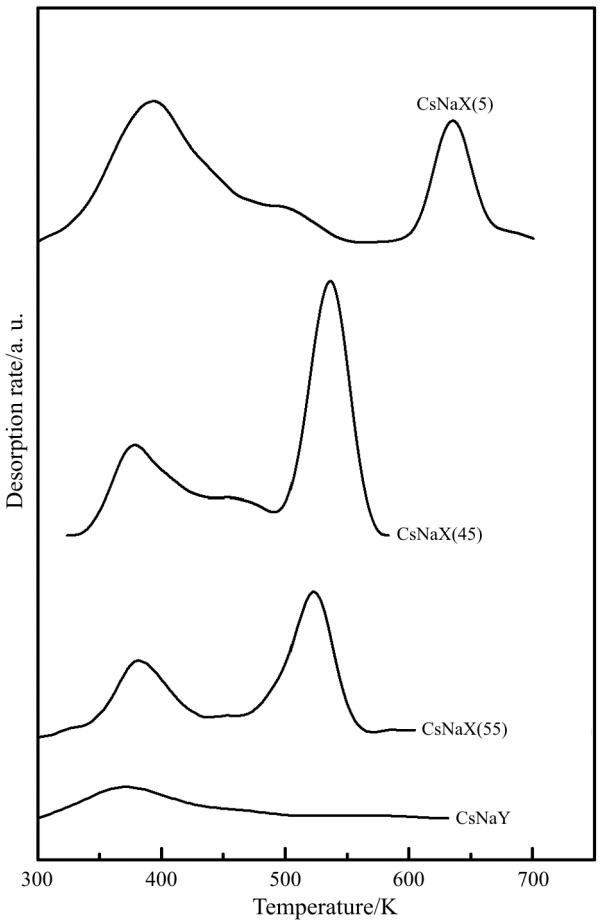

Fig. 3 Desorption profiles of CO_2 on Cs^+ ion-exchanged zeolites (10 K min^{-1})

In case of NaX and X type zeolites exchanged with Cs^+ ions an additional desorption peak appears above 500 K (Figs 1 and 3). For CsNaX(45) zeolite sample it was found that the peak intensity increases with longer adsorption times and higher adsorption temperatures as can be seen in Figs 4 and 5. The increasing intensity of the desorption peak at higher temperatures is accompanied by a decrease of the desorbed amount at lower temperatures. These findings indicate that different adsorption states of CO_2 influence each other. One can conclude that the formation of the strongly adsorbed CO_2 is an activated process.

Table 2 Desorbed CO_2 amounts in different temperature ranges

Zeolite	300–500 K/ μmol g^{-1}	500–800 K/ μmol g^{-1}	Total/ μmol g^{-1}
Li-LSX	1.2	–	1.2±0.1
NaX	32.6	2.5	35.1±0.5
KNaX	26.7	–	26.7
RbNaX	15.8	–	15.8
CsNaX(5)	7.9	2.5	10.4
CsNaX(45)	3.6	5.1	8.7
CsNaX(55)	2.6	3.4	6.0
NaY	2.9	–	2.9
CsNaY	1.7	–	1.7

The observed desorption profiles $r_d(T)$ were analyzed by considering a first order desorption process with a distribution function $f(E)$ of the effective desorption energy E [18, 19]:

$$r_d(T) = -\frac{d\theta}{dt}(T) = \\ = A\int_{E_{min}}^{E_{max}} \theta_{loc}(E,T)\exp\left(-\frac{E}{RT}\right) f(E)dE \quad (1)$$

Here θ is the average coverage or loading, and A is an effective pre-exponential factor. θ_{loc} is the coverage of adsorption sites with desorption energy E. E_{min} and E_{max} are the limits of the desorption energy range. The estimation of the desorption energy distribution function from experimental TPD data, i.e. the solution of Eq. (1) requires the knowledge of the pre-exponential factor A. In a previous paper [20] it could be shown that taking into account desorption curves of different heating rates desorption energy distribution functions can be calculated without any a priori knowledge about A by using an extended integral

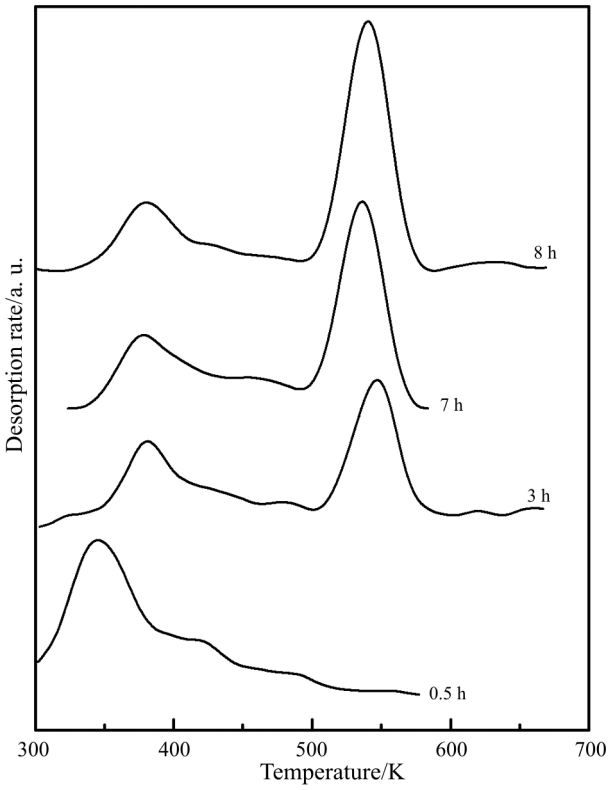

Fig. 4 Desorption profiles of CO_2 on CsNaX(45) after adsorption at 298 K using different flushing times with helium

equation. All calculations were carried out by the program INTEG, which involves a regularization method for solving the integral equation [18, 20].

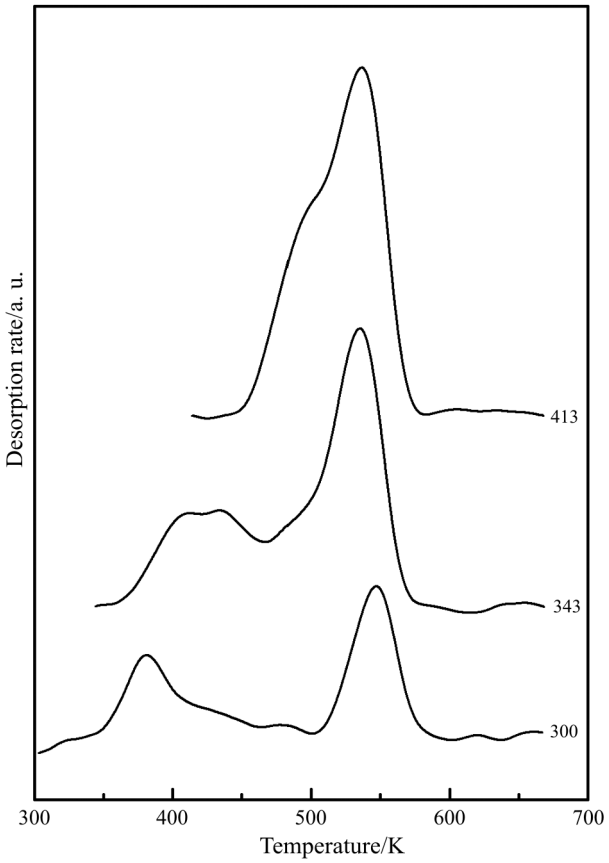

Fig. 5 Desorption profiles of CO_2 on CsNaX(45) after adsorption at different temperatures

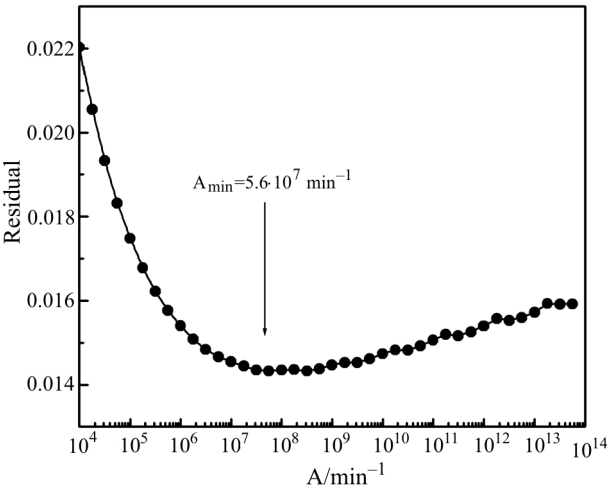

Fig. 6 Dependence of the residual of the regularization on the pre-exponential factor for CO_2-TPD on NaX using desorption curves with different heating rates

The residual of the regularization in dependence on the pre-exponential factor shows for CO_2-TPD on NaX a minimum at $A=5.6\cdot10^7$ min^{-1} ($\ln A=17.8\pm0.6$) (Fig. 6) by using several desorption curves at different heating rates (α=2–20 K min^{-1}). This value of A corresponds to the optimal description of all desorption curves with the calculated desorption energy distribution function.

The pre-exponential factor can be also determined by the relationship between the peak-maximum temperature and the heating rate even if the desorption energy depends on the coverage [21, 22]. Figure 7 shows the corresponding plot for the high temperature peak of CO_2 desorption on NaX. By linear fitting a pre-exponential factor of $A=4.8\cdot10^7$ min^{-1} ($\ln A=17.7\pm0.8$) was obtained. The estimation for the low temperature peak results in a value of $A=4.0\cdot10^7$ min^{-1} ($\ln A=17.5\pm1.7$). The differences between the three obtained values correspond to the accuracy of estimation of this parameter. Therefore, a constant value of $5\cdot10^7$ min^{-1} was used for the calculation of the distribution function of the desorption profile in the temperature range between 300 and 700 K.

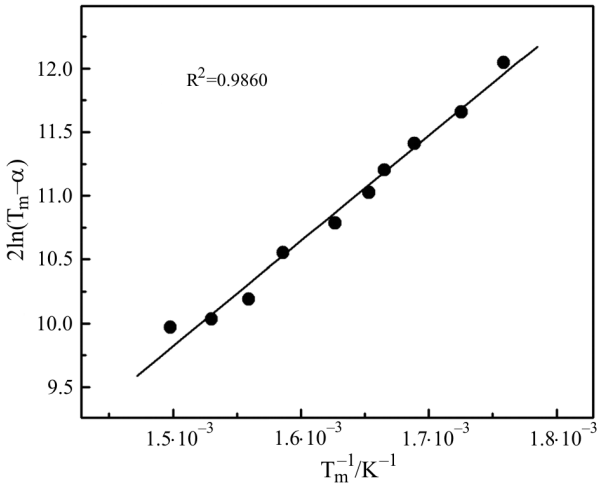

Fig. 7 Plot of $2\ln(T_m-\alpha)$ *vs.* $1/T_m$ of the high temperature peak of CO_2 desorption on NaX

The calculated desorption energy distribution function for NaX is presented in Fig. 8. The width of the bimodal distribution function of about 60 kJ mol^{-1} shows clearly the energetic heterogeneity of the CO_2-zeolite interaction. In case of Cs^+ ion-exchanged X type zeolites the calculation also result in a bimodal distribution. For KNaX and RbNaX zeolites distribution functions of the effective desorption energy with one pronounced maximum at about 60 kJ mol^{-1} were obtained. In Table 3 the energy values of the maxima of all desorption energy distributions are summarized. For NaX the obtained desorption energies (50–110 kJ mol^{-1}) are higher than isosteric heats of adsorption of CO_2 at

Table 3 Energy values of the maxima of desorption energy distribution functions

Zeolite	Peak 1/kJ mol^{-1}	Peak 2/kJ mol^{-1}
NaX	59±6	99±6
KNaX	59	–
RbNaX	58	–
CsNaX(5)	60	100
CsNaX(45)	58	85

lower coverages calculated from adsorption isotherms (limit of zero coverage: 47–50 kJ mol^{-1}) [5, 6]. Higher initial heats of adsorption (up to 70 kJ mol^{-1}) were only obtained by calorimetric measurements at higher adsorption temperatures (343 K) [3] indicating that the formation of stronger adsorbed carbon dioxide is a slow and activated process. This finding is in agreement with the presented TPD results.

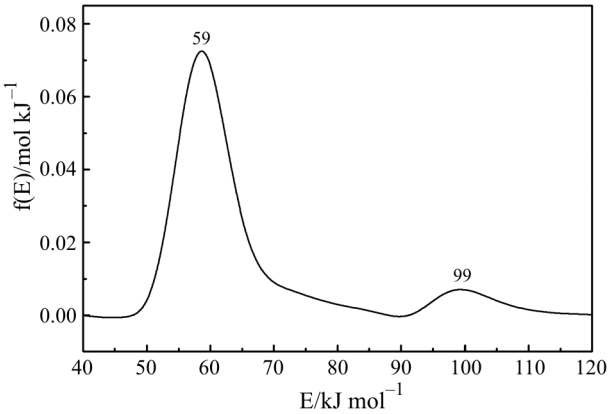

Fig. 8 Desorption energy distribution function of CO_2 on NaX

In order to characterize the adsorption state of carbon dioxide on investigated zeolites DRIFT spectroscopic studies were carried out. In Figs 9 and 10 DRIFT spectra of CsNaX(45) and NaX are shown. The ν_3 vibration (slightly shifted to the 2349 cm^{-1} value for free CO_2) of linearly adsorbed carbon dioxide in an end-on configuration to a cation (e.g. [17, 23, 24]) could not be observed (Fig. 9). It is not a surprising result because the present adsorption conditions do not allow adsorption of weakly interacting CO_2, but result only in a smaller uptake of stronger adsorbed carbon dioxide. On CsNaX(45) different pairs of bands were obtained in the wavenumber region between 1800 and 1300 cm^{-1} depending on the adsorption temperature. After adsorption at 298 K two pairs of bands appear at 1679 and 1337 and at 1653 and 1387 cm^{-1}, respectively. Whereas after adsorption at 413 K only one pair of bands at 1649 and 1381 cm^{-1} is observed. These bands can be assigned to carbonate structures of adsorbed CO_2 coordinated to an extra-framework cation and a framework oxygen atom [25–27]. The splitting of the ν_3 vibration of free ion CO_3^{2-} ($\nu_3 \approx$1440–1450 cm^{-1}) into two bands is caused by lowering the symmetry due to the interaction of CO_2 with the zeolite to built the carbonate structure [28]. The two pairs of bands with different extent of splitting represent two bent configurations of adsorbed carbon dioxide within zeolite cavities in different environments. After adsorption at 413 K bands only appear at 1649 and 1381 cm^{-1}. One can conclude that these bands of lower splitting ($\Delta\nu$=286 cm^{-1}) correspond to adsorbed CO_2 of higher thermal stability which desorbs above 450 K with an average desorption energy of 85 kJ mol^{-1} (Fig. 3, Table 3). The other pair of bands with higher splitting ($\Delta\nu$=342 cm^{-1}) can be assigned to adsorbed CO_2 desorbing at lower temperatures between 300 and 450 K with a desorption energy of about 60 kJ mol^{-1}. The stronger interaction of a part of adsorbed CO_2 on CsNaX zeolites with higher Cs^+ ion content should be mainly caused by the higher partial negative charge (higher basicity) of the framework oxygen atoms of these zeolites [29]. The conclusion is supported by TPD results on CsNaY. This zeolite with a lower basicity of the oxygen atoms due to the lower aluminium content shows no desorption of CO_2 at higher temperatures (Fig. 3).

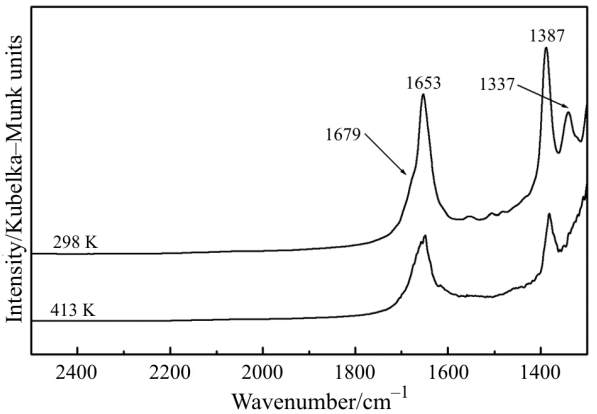

Fig. 9 DRIFT spectra of CsNaX(45) after adsorption of CO_2 at 298 and 413 K

Besides two pairs of bands at 1711/1362 cm^{-1} ($\Delta\nu$=347 cm^{-1}) and at 1690/1375 cm^{-1} ($\Delta\nu$=315 cm^{-1}) a new pair of bands at 1482 and 1426 cm^{-1} ($\Delta\nu$=56 cm^{-1}) appears after adsorption of CO_2 on NaX (Fig. 10). These bands were already observed for carbon dioxide adsorption on NaX and sometimes on dehydrated and partially hydrated Ca^{2+} ion-exchanged X and Y type zeolites. It can be related to 'true' carbonate structures in an almost symmetrical environment which possess a higher thermal stability of the adsorption structure [25–27]. Thus the high-temperature peak of CO_2-TPD at 670 K on NaX and CsNaX(5) with a desorption energy of

100 kJ mol^{-1} can be related to this 'true' carbonate structure (Figs 1 and 3, Table 3). This assignment is also supported by results of temperature-programmed DRIFTS studies (5 K min^{-1}) which have been shown that the pairs at 1711/1362 and at 1690/1375 cm^{-1} disappear at about 420 K. Whereas the bands of the other pair with lower splitting disappear at about 520 K.

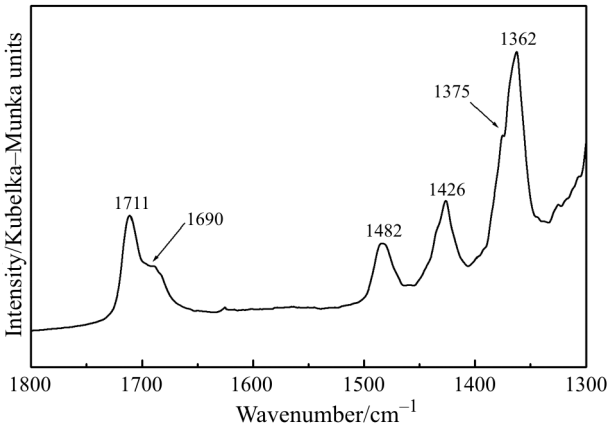

Fig. 10 DRIFT spectra of NaX after adsorption of CO_2 at 298 K

The presented CO_2-TPD results are, to our best knowledge, the first experimental evidence of carbonate species on faujasite type zeolites next to infrared spectroscopic studies. However, a clarification of the molecular structure should be a difficult task, because only a small amount of these species exist.

Acknowledgements

This work was partially supported by the Deutsche Forschungsgemeinschaft, Graduate College 'Physical Chemistry of Interfaces'. We thank Dr. H. Toufar, Tricat Zeolites GmbH (Bitterfeld, Germany) for providing the Li-LSX zeolite.

References

1 V. P. Shiralkar and S. B. Kulkarni, Zeolites, 4 (1984) 329.
2 V. P. Shiralkar and S. B. Kulkarni, Zeolites, 5 (1985) 37.
3 D. Amari, J. M. Lopez Cuesta, N. P. Nguyen, R. Jerrentrup and J. L. Ginoux, J. Thermal Anal., 38 (1992) 1005.
4 P. N. Joshi and V. P. Shiralkar, J. Phys. Chem., 97 (1993) 619.
5 J. A. Dunne, M. Rao, S. Sircar, R. J. Gorte and A. L. Myers, Langmuir, 12 (1996) 5896.
6 D. Shen and M. Bülow, Microporous Mesoporous Mater., 22 (1998) 237.
7 Z.-M. Wang, T. Arai and M. Kumagai, Energy Fuels, 12 (1998) 1055.
8 Y. Zou and A. E. Rodrigues, Adsorpt. Sci. Technol., 19 (2001) 255.
9 A. L. Pulin, A. A. Fomkin, V. A. Sinitsyn and A. A. Pribylov, Russ. Chem. Bull., Int. Ed., 50 (2001) 60.
10 J.-S. Lee, J.-H. Kim, J.-T. Kim, J.-K Suh, J.-M. Lee and C.-H. Lee, J. Chem. Eng. Data, 47 (2002) 1237.
11 R. V. Siriwardane, M.-S. Shen and E. P. Fisher, Energy Fuels, 17 (2003) 571.
12 A. Auroux and A. Gervasini, J. Phys. Chem., 94 (1990) 6371.
13 H. Tsuji, F. Yagi and H. Hattori, Chem. Lett., (1991) 1881.
14 P. Käßner and M. Baerns, Appl. Catal., A: General, 139 (1996) 107.
15 H. Förster, H. Fuess, E. Geidel, B. Hunger, H. Jobic, C. Kirschhock, O. Klepel and K. Krause, Phys. Chem. Chem. Phys., 1 (1999) 593.
16 B. Hunger, O. Klepel, C. Kirschhock, M. Heuchel, H. Toufar and H. Fuess, Langmuir, 15 (1999) 5937.
17 V. B. Kazansky, V. Yu. Borovkov, A. I. Serykh and M. Bülow, Phys. Chem. Chem. Phys., 1 (1999) 3701.
18 M. von Szombathely, P. Bräuer and M. Jaroniec, J. Comput. Chem., 13 (1992) 17.
19 B. Hunger, M. von Szombathely, J. Hoffmann and P. Bräuer, J. Thermal Anal., 44 (1995) 293.
20 K. Koch, B. Hunger, O. Klepel and M. Heuchel, J. Catal., 172 (1997) 187.
21 B. Hunger and J. Hoffmann, Thermochim. Acta, 106 (1986) 133.
22 P. T. Dawson and Y. K. Peng, Surf. Sci., 33 (1972) 565.
23 B. Bonelli, B. Onida, B. Fubini, C. Otero Areán and E. Garrone, Langmuir, 16 (2000) 4976.
24 F. X. Llabrés i Xamena and A. Zecchina, Phys. Chem. Chem. Phys., 4 (2002) 1978.
25 P. A. Jacobs, F. H. van Cauwelaert, E. F. Vansant and J. B. Uytterhoeven, J. Chem. Soc., Faraday Trans. I, 69 (1973) 1056.
26 P. A. Jacobs, F. H. van Cauwelaert and E. F. Vansant, J. Chem. Soc., Faraday Trans. I, 69 (1973) 2130.
27 L. Bertsch and H. W. Habgood, J. Phys. Chem., 67 (1963) 1621.
28 A. A. Davydov, 'Infrared Spectroscopy of Adsorbed Species on the Surface of Transition Metal Oxides', John Wiley and Sons, New York 1990, p. 38.
29 R. Heidler, G. O. A. Janssens, W. J. Mortier and R. A. Schoonheydt, J. Phys. Chem., 100 (1996) 19728.